Bragg spectroscopy of an accelerating condensate with solitary-wave behavior

K. J. Challis* and R. J. Ballagh

Department of Physics, University of Otago, P. O. Box 56, Dunedin, New Zealand
(Received 7 October 2004; published 18 March 2005)

We present a theoretical treatment of Bragg spectroscopy of an accelerating condensate in a solitary-wave state. Our treatment is based on the Gross-Pitaevskii equation with an optical potential representing the Bragg pulse and an additional external time-dependent potential generating the solitary-wave behavior. By transforming to a frame translating with the condensate, we derive an approximate set of equations that can be readily solved to generate approximate Bragg spectra. Our analytic method is accurate within a well-defined parameter regime and provides physical insight into the structure of the spectra. We illustrate our formalism using the example of Bragg spectroscopy of a condensate in a time-averaged orbiting potential trap.

I. INTRODUCTION

Bragg spectroscopy has proved to be a precise and versatile technique for measuring a variety of properties of a Bose-Einstein condensate, including the momentum distribution [1] and coherence functions [2]. A theoretical proposal has been made to use Bragg spectroscopy to provide a signature of a vortex state in a condensate [3], and recently the technique has been suggested as a means for characterizing superfluid pairing in fermionic systems [4].

The theoretical description of Bragg spectroscopy of a condensate is well established and Blakie *et al.* [5], for example, have shown that a mean-field treatment using the Gross-Pitaevskii equation is an appropriate formalism. Unfortunately, numerically calculating a Bragg spectrum using the Gross-Pitaevskii equation is highly computationally intensive and may not readily yield a physical interpretation of the system.

In this paper we present a treatment of Bragg spectroscopy of a condensate which is accelerating in the form of a solitary wave due to the influence of an external time-dependent trapping potential. Solitary-wave behavior occurs only for a certain class of potentials, but is not uncommon. A simple example is the dipole oscillation of a condensate in a harmonic trap. Our method is based on transforming to the frame of reference where the condensate is stationary, allowing us to establish a relatively simple set of equations that can be readily solved to give approximate Bragg spectra. We also obtain an analytic approximation to the spectrum, which provides physical insight into its structure.

The paper is organized as follows. In Sec. II we describe our theoretical formalism, introducing solitary-wave solutions of the Gross-Pitaevskii equation and transforming the equation to the translating frame. We outline a simple two-state momentum-space formalism which can be used to generate approximate Bragg spectra for a general solitary wave, and we determine the validity regime in which such spectra are accurate. In Sec. III we use the methods of Sec. II to treat Bragg spectroscopy of a condensate undergoing micromotion

in a time-averaged orbiting potential trap. We demonstrate the utility of our approximate solutions by comparing them with Bragg spectra calculated by simulating the Gross-Pitaevskii equation. Bragg spectroscopy in a time-averaged orbiting potential trap has been investigated experimentally [6] and our treatment provides quantitative agreement with full theoretical calculations and qualitative agreement with the experimental results [7].

II. BRAGG SPECTROSCOPY OF A SOLITARY WAVE

Our theoretical treatment is based on solving the Gross-Pitaevskii equation for a condensate with wave function $\psi(\mathbf{r},t)$, in the presence of a time-dependent external trapping potential and a Bragg pulse, i.e.,

$$i\frac{\partial}{\partial t}\psi(\mathbf{r},t) = [-\nabla^2 + V(\mathbf{r},t) + V_{\mathrm{opt}}(\mathbf{r},t) + C|\psi(\mathbf{r},t)|^2]\psi(\mathbf{r},t).$$

(1)

We have chosen to present our discussion in terms of dimensionless units where the time scale is given by the inverse of a characteristic trap frequency ω_x (e.g., as defined in Sec. II A 1) and the position scale is $x_0 = \sqrt{\hbar/2m\omega_x}$ (where m is the mass of an atom). The external trapping potential $V(\mathbf{r},t)$ can be decomposed without loss of generality as

$$V(\mathbf{r},t) = V(\mathbf{r}) + G(\mathbf{r},t),$$

(2)

and the optical potential generated by the Bragg pulse is

$$V_{\mathrm{opt}}(\mathbf{r},t) = \frac{1}{2}U_0\cos(\mathbf{q}\cdot\mathbf{r} - \omega t),$$

(3)

where $\mathbf{q}$ and ω are, respectively, the wave-vector difference and the frequency difference between the two laser beams forming the Bragg pulse [8]. The dimensionless nonlinearity coefficient C is defined in terms of the number of condensed atoms N and the s-wave scattering length a, i.e.,

$$C = \frac{4\pi\hbar a N}{m\omega_x x_0^3}.$$

(4)

*Electronic address: kchallis@physics.otago.ac.nz

A. Solitary-wave solutions

Solitary-wave solutions to the Gross-Pitaevskii equation in the absence of the optical potential [Eq. (1) with $U_0=0$] exist for particular forms of the external potential $V(\mathbf{r},t)$ of Eq. (2). Such solutions, which evolve in three dimensions without changing shape, have been discussed previously [9–11] and have the form

$$\psi_{\mathrm{SW}}(\mathbf{r},t) = \xi(\mathbf{r} - \bar{\mathbf{r}}(t))e^{-i\mu t + iS(\mathbf{r},t)}, \qquad (5)$$

where the envelope wave function $\xi(\mathbf{r})$ is an eigenstate of the time-independent Gross-Pitaevskii equation with the time-independent trapping potential $V(\mathbf{r})$ and chemical potential μ, i.e.,

$$\mu\xi(\mathbf{r}) = \left[-\nabla^2 + V(\mathbf{r}) + C|\xi(\mathbf{r})|^2\right]\xi(\mathbf{r}). \qquad (6)$$

The position offset in the envelope wave function is

$$\bar{\mathbf{r}}(t) = \int \psi_{\mathrm{SW}}^*(\mathbf{r},t)\mathbf{r}\psi_{\mathrm{SW}}(\mathbf{r},t)d\mathbf{r} - \int \xi^*(\mathbf{r})\mathbf{r}\xi(\mathbf{r})d\mathbf{r}. \qquad (7)$$

The phase $S(\mathbf{r},t)$ is determined by substituting the solitary-wave solution (5) into the time-dependent Gross-Pitaevskii equation. We restrict our discussion to solutions where the velocity of the envelope $\xi(\mathbf{r}-\bar{\mathbf{r}}(t))$, equal to the center-of-mass velocity $d\bar{\mathbf{r}}(t)/dt$, is proportional to the gradient of $S(\mathbf{r},t)$ [in our units $2\nabla S(\mathbf{r},t)$]. (For further details regarding the derivation of $S(\mathbf{r},t)$ see Refs. [9,11].) We find that

$$S(\mathbf{r},t) = \frac{1}{2}\mathbf{r} \cdot \frac{d\bar{\mathbf{r}}(t)}{dt} + \frac{1}{4}\int_{t_0}^{t}\left[\bar{\mathbf{r}}^2(\tau) - \left(\frac{d\bar{\mathbf{r}}(\tau)}{d\tau}\right)^2\right]d\tau, \qquad (8)$$

where t_0 is chosen for convenience such that any constant (i.e., global) phase in $\psi_{\mathrm{SW}}(\mathbf{r},t)$ is set to zero. The center-of-mass motion of the solitary-wave solutions can be shown to obey a form of Ehrenfest's theorem,

$$\frac{1}{2}\frac{d^2\bar{\mathbf{r}}(t)}{dt^2} = -\nabla F(\mathbf{r},t), \qquad (9)$$

where

$$F(\mathbf{r},t) = V(\mathbf{r},t) - V(\mathbf{r} - \bar{\mathbf{r}}(t)). \qquad (10)$$

For solitary-wave solutions to exist the function $F(\mathbf{r},t)$ must yield a solution to Eq. (9) and, therefore, can be at most linear in $\mathbf{r}$.

1. Harmonic trap

In Bose-condensed systems it is most common that the time-independent trapping potential $V(\mathbf{r})$ is harmonic, i.e.,

$$V_{\mathrm{H}}(\mathbf{r}) = \frac{1}{4}(x^2 + y^2 + \lambda^2 z^2), \qquad (11)$$

with frequency ω_x in the x-y plane (in SI units), aspect ratio λ, and where $\mathbf{r}=(x,y,z)$. In the absence of the Bragg pulse ($U_0=0$), the Gross-Pitaevskii equation (1) has solitary-wave solutions provided that $G(\mathbf{r},t)$ has the particular form such that Eq. (9) is satisfied, i.e.,

$$G(\mathbf{r},t) = \mathbf{g}_1(t) \cdot \mathbf{r} + g_2(t), \qquad (12)$$

where $\mathbf{g}_1(t)$ and $g_2(t)$ are arbitrary functions of t.

Solitary-wave behavior is not uncommon in condensates confined by a harmonic trap. Some examples include the dipole oscillation [$\mathbf{g}_1(t)=\mathbf{0}$], the motion resulting from translations of the trap due to the effect of noise [$\mathbf{g}_1(t)\neq\mathbf{0}$], and the solitary-wave micromotion of a condensate in a time-averaged orbiting potential trap (to be discussed in Sec. III). Bragg spectroscopy is a highly velocity-sensitive technique and while the Bragg spectrum of a solitary-wave solution with constant velocity is relatively straightforward to predict, the Bragg spectrum of an accelerating solitary-wave condensate [with $d\bar{\mathbf{r}}(t)/dt$ a function of t] can be complicated and it is the latter case that is the focus of this paper.

B. Translating frame

We begin our treatment of Bragg spectroscopy in a time-dependent external trapping potential by transforming to the frame translating such that the condensate center-of-mass is stationary in that frame. While numerical solutions of the Gross-Pitaevskii equation can be calculated in the laboratory frame, the description of the system in the translating frame, where the condensate is at rest, allows simple approximate methods and a physical interpretation to be developed since the only time dependence for the system in the translating frame appears via an effective optical potential.

A general quantum-mechanical transformation to an accelerating translating frame has been given earlier [11]. For the particular case we are interested in, of solitary-wave motion, the translation in coordinate space is defined by setting the coordinates of the new frame to be

$$\mathbf{R} = \mathbf{r} - \bar{\mathbf{r}}(t), \qquad (13)$$

where we denote the components of $\mathbf{R}$ to be (X,Y,Z). The momentum in the translating frame is derived by differentiating Eq. (13) yielding

$$\mathbf{P} = \mathbf{p} - \frac{1}{2}\frac{d\bar{\mathbf{r}}(t)}{dt}, \qquad (14)$$

where we have used the fact that in our dimensionless units $\mathbf{p}=\mathbf{v}/2$. The wave function in the translating frame is

$$\psi^t(\mathbf{R},t) = e^{(-1/2)i\mathbf{R}\cdot d\bar{\mathbf{r}}(t)/dt}\psi(\mathbf{r},t), \qquad (15)$$

facilitating the momentum translation of Eq. (14).[1] The Gross-Pitaevskii equation in the translating frame can now be derived by transforming Eq. (1) using Eqs. (13) and (15) to yield

---

[1] Unlike the derivation in Ref. [11] we do not assume that $\bar{\mathbf{r}}(t) \cdot d\bar{\mathbf{r}}(t)/dt=0$. However, in the case where the unitary operators that generate the position and momentum translations of Eqs. (13) and (14) do not commute, the additional factor in the unitary transformation to an accelerating translating frame is a time-dependent phase which can be removed in an interaction picture.

$$i\frac{\partial}{\partial t}\psi^t(\mathbf{R},t) = \left[-\nabla_{\mathbf{R}}^2 + W^t(\mathbf{R},t) + V_{\text{opt}}^t(\mathbf{R},t)\right.$$

$$\left. + C|\psi^t(\mathbf{R},t)|^2\right]\psi^t(\mathbf{R},t). \qquad (16)$$

In Eq. (16) we have denoted

$$\nabla_{\mathbf{R}} = \left(\frac{\partial}{\partial X}, \frac{\partial}{\partial Y}, \frac{\partial}{\partial Z}\right), \qquad (17)$$

and the optical potential in the translating frame is

$$V_{\text{opt}}^t(\mathbf{R},t) = \frac{1}{2}U_0\cos[\mathbf{q}\cdot\mathbf{R} + \mathbf{q}\cdot\bar{\mathbf{r}}(t) - \omega t]. \qquad (18)$$

The potential denoted $W^t(\mathbf{R},t)$ is the sum of the external trapping potential in the translating frame and additional terms due to the momentum translation, i.e.,

$$W^t(\mathbf{R},t) = V(\mathbf{R} + \bar{\mathbf{r}}(t),t) + \frac{1}{2}\mathbf{R}\cdot\frac{d^2\bar{\mathbf{r}}(t)}{dt^2} - \frac{1}{4}\left(\frac{d\bar{\mathbf{r}}(t)}{dt}\right)^2. \qquad (19)$$

By taking the gradient of Eq. (19) and making a comparison with Eq. (9) we find that

$$\nabla_{\mathbf{R}}W^t(\mathbf{R},t) = \nabla_{\mathbf{R}}V(\mathbf{R}) \qquad (20)$$

and, therefore,

$$W^t(\mathbf{R},t) = V(\mathbf{R}) + A(t), \qquad (21)$$

where $A(t)$ is a function only of time. Defining an interaction picture by

$$\psi^T(\mathbf{R},t) = \psi^t(\mathbf{R},t)\exp\left(i\int A(t)dt\right), \qquad (22)$$

the Gross-Pitaevskii equation becomes

$$i\frac{\partial}{\partial t}\psi^T(\mathbf{R},t) = \left[-\nabla_{\mathbf{R}}^2 + V(\mathbf{R}) + V_{\text{opt}}^t(\mathbf{R},t)\right.$$

$$\left. + C|\psi^T(\mathbf{R},t)|^2\right]\psi^T(\mathbf{R},t), \qquad (23)$$

which shows that in the translating frame all the explicit time dependence of the system is contained within the optical potential term [see Eq. (18)]. When the Bragg pulse is turned off, stationary solutions of Eq. (23) are of the form

$$\psi_{\text{SW}}^T(\mathbf{R},t) = \xi(\mathbf{R})e^{-i\mu t}, \qquad (24)$$

which are solitary-wave solutions in the laboratory frame with center-of-mass motion governed by Eq. (9).

C. Simple momentum formalism

A theoretical formalism for describing Bragg spectroscopy of a stationary condensate has been developed by Blakie *et al.* [8]. Those authors derived an analytic treatment of Bragg scattering, for the case where $C=0$, using an approximate two-state momentum-space model to consider condensates released from a harmonic trap at the instant that the Bragg pulse is applied. Their treatment provides a simple approximate method for generating Bragg spectra which,

within a given parameter regime, are in quantitative agreement with full calculations of the Gross-Pitaevskii equation. Here we extend that model to describe Bragg spectroscopy of condensates moving with solitary-wave behavior.

Following broadly the approach of Blakie *et al.* [8] we place three restrictions on the system. First, mean-field effects are neglected by taking $C=0$. Our treatment of the non-linear term is detailed in Sec. II D. Second, the time-independent trapping potential $V(\mathbf{r})$ is neglected while retaining the time-dependent $G(\mathbf{r},t)$. This means that the condensate center-of-mass motion is still governed by Eq. (9) but the condensate is no longer confined about its center of mass. When neglecting atomic interactions, removing the trap $V(\mathbf{r})$ does not alter the momentum distribution of the unscattered condensate, whereas the condensate part scattered by the Bragg pulse is no longer decelerated. Provided that the Bragg pulse length is short compared to the oscillation period of atoms confined by $V(\mathbf{r})$, the effect of the confining potential on the Bragg spectrum is negligible. In some experimental systems it may be possible to apply $V(\mathbf{r})$ and $G(\mathbf{r},t)$ independently so that $V(\mathbf{r})$ can be turned off when the Bragg pulse is applied. Third, for simplicity, we choose the wave vector $\mathbf{q}$ of the optical potential to lie along the x axis such that $\mathbf{q}\cdot\mathbf{R}=qX$ and the optical potential (18) becomes

$$V_{\text{opt}}^t(X,t) = \frac{1}{2}U_0\cos[qX + q\bar{x}(t) - \omega t]. \qquad (25)$$

This can be done without loss of generality for the case where $V(\mathbf{r})$ is turned off. Finally then, within these restrictions, the wave function $\psi^T(\mathbf{R},t)$ is separable and denoting the product wave function in X by $\psi^T(X,t)$ it is possible to reduce the analysis of the system to one dimension without loss of generality [8].

We begin by transforming the one-dimensional equivalent of Eq. (23), with $C=0$ and $V(\mathbf{R})=0$, into momentum space using the Fourier integral

$$\phi^T(K,t) = \frac{1}{\sqrt{2\pi}}\int \psi^T(X,t)e^{-iKX}dX, \qquad (26)$$

to give

$$i\frac{\partial}{\partial t}\phi^T(K,t) = K^2\phi^T(K,t) + \frac{1}{4}U_0[e^{-i[\omega t - q\bar{x}(t)]}\phi^T(K-q,t)$$

$$+ e^{i[\omega t - q\bar{x}(t)]}\phi^T(K+q,t)]. \qquad (27)$$

Next, we partition momentum space into bins of width q, centered around the Bragg orders $K=nq$, where n is integer. That is achieved by expressing the wave function $\phi^T(K,t)$ as a set of wave functions $\tilde{\phi}_n^T(\tilde{K},t)$, each defined only within bin n of the partitioned momentum space, i.e.,

$$\tilde{\phi}_n^T(\tilde{K},t) = \phi^T(K,t), \qquad (28)$$

where

$$\widetilde{K}: \left(n - \frac{1}{2}\right)q < K < \left(n + \frac{1}{2}\right)q. \tag{29}$$

The description of the system is simplified by defining $\kappa = \widetilde{K} - nq$ and writing

$$\phi_n^{\mathrm{T}}(\kappa, t) = \widetilde{\phi}_n^{\mathrm{T}}(\widetilde{K}, t) e^{in[\omega t - q\bar{x}(t)]}, \tag{30}$$

where κ varies from $-q/2$ to $q/2$, for every bin. The momentum-space Schrödinger equation can then be written as an infinite set of equations coupling wave functions of consecutive bins,

$$i\frac{\partial}{\partial t}\phi_n^{\mathrm{T}}(\kappa, t) = \omega_n(\kappa, t)\phi_n^{\mathrm{T}}(\kappa, t) + \frac{1}{4}U_0[\phi_{n-1}^{\mathrm{T}}(\kappa, t) + \phi_{n+1}^{\mathrm{T}}(\kappa, t)], \tag{31}$$

where

$$\omega_n(\kappa, t) = (\kappa + nq)^2 - n\omega + nq\frac{d\bar{x}(t)}{dt}. \tag{32}$$

Equation (31) is identical to that derived by Blakie *et al.* [8] for a stationary untrapped condensate, with the exception of an additional time dependence appearing in $\omega_n(\kappa, t)$. The additional term $nq\,d\bar{x}(t)/dt$ is due to the momentum of the condensate in the laboratory frame [see Eq. (14)] and has previously been referred to as the Doppler term [6].

To determine the Bragg spectrum of an accelerating condensate we calculate the population in the first Bragg order ($n = +1$ bin) as a function of the frequency difference ω in the optical potential. In the translating frame this is given by

$$P_{+1}(\omega, t) = \int_{-q/2}^{q/2} |\phi_{+1}^{\mathrm{T}}(\kappa, t)|^2 d\kappa, \tag{33}$$

corresponding in the laboratory frame to

$$P_{+1}(\omega, t) = \int_{[q + d\bar{x}(t)/dt]/2}^{[3q + d\bar{x}(t)/dt]/2} |\phi(k, t)|^2 dk, \tag{34}$$

where $\phi(k, t)$ is defined by

$$\phi(k, t) = \frac{1}{\sqrt{2\pi}} \int \psi(x, t) e^{-ikx} dx \tag{35}$$

in terms of the wave function in the laboratory frame $\psi(x, t)$, and the limits of integration in Eq. (34) account for the solitary-wave center-of-mass motion of the condensate.

Solving Eq. (31), in order to calculate $\phi_{+1}^{\mathrm{T}}(\kappa, t)$, is no more straightforward than solving the full Schrodinger equation. Again following the treatment of Blakie *et al.* [8] the problem becomes readily tractable if we assume that in the region of interest, where first-order Bragg scattering is strong, only the $n = 0$ and $+1$ momentum wave functions are substantially populated. In this "two-state model" Eq. (31) reduces to

$$i\frac{\partial}{\partial t}\begin{bmatrix} \phi_0^{\mathrm{T}}(\kappa, t) \\ \phi_{+1}^{\mathrm{T}}(\kappa, t) \end{bmatrix} = \begin{bmatrix} \omega_0(\kappa) & \frac{1}{4}U_0 \\ \frac{1}{4}U_0 & \omega_0(\kappa) + \Delta_{0\to+1}(\kappa, t) \end{bmatrix} \begin{bmatrix} \phi_0^{\mathrm{T}}(\kappa, t) \\ \phi_{+1}^{\mathrm{T}}(\kappa, t) \end{bmatrix}, \tag{36}$$

where $\omega_0(\kappa) = \kappa^2$ and

$$\Delta_{0\to+1}(\kappa, t) = q^2 + 2\kappa q - \omega + q\frac{d\bar{x}(t)}{dt}. \tag{37}$$

Equation (36) can be solved easily by numerical means and its solution accurately describes the system when $n \neq 0, +1$ populations are negligible. The validity conditions for Eq. (36) are now derived.

1. Validity of the two-state model

The two-state model is valid when only the $n = 0$ and $+1$ bins are significantly populated. Accounting for two-photon transitions only (which couple consecutive bins) the detuning for the transition from bin n to bin m is defined by

$$\Delta_{n\to m}(\kappa, t) = \omega_m(\kappa, t) - \omega_n(\kappa, t), \tag{38}$$

where $|m - n| = 1$. We define a transition to be on resonance when the magnitude of the detuning is less than $U_0/2$ (determined by the power-broadened width [8]). Thus, the first-order Bragg transition (between the $n = 0$ and $+1$ bins) will be resonant for some part of the initial condensate momentum distribution over the frequency range

$$\omega > q^2 + q\left.\frac{d\bar{x}(t)}{dt}\right|_{\mathrm{min}} - \sigma q - \frac{1}{2}U_0 \tag{39}$$

and

$$\omega < q^2 + q\left.\frac{d\bar{x}(t)}{dt}\right|_{\mathrm{max}} + \sigma q + \frac{1}{2}U_0, \tag{40}$$

where σ is the full momentum width of the condensate. We have chosen to use the $1/e$ condensate momentum width and the extreme values of $d\bar{x}(t)/dt$ in order to yield the largest possible transition width and, therefore, the strictest condition for the two-state validity. Within the frequency range defined by Eqs. (39) and (40) we require that the transitions to neighboring bins ($n = -1$ and $+2$) are not resonant, i.e., $|\Delta_{-1\to 0}(\kappa, t)| > U_0/2$ and $|\Delta_{+1\to+2}(\kappa, t)| > U_0/2$. Those conditions are satisfied when

$$U_0 < 2q(q - \sigma - \delta_p), \tag{41}$$

where $2\delta_p = d\bar{x}(t)/dt|_{\mathrm{max}} - d\bar{x}(t)/dt|_{\mathrm{min}}$. Note that Eq. (41) requires $\sigma < q$, which also ensures that momentum wave functions of consecutive bins do not overlap.

The discussion leading to Eq. (41) does not account for higher-order processes. It is possible for $2m$-photon processes to transfer population from the $n = 0$ to the $n = m$ bin, without intermediate bins accumulating significant population. However, provided the Rabi period for such processes is significantly longer than the Bragg pulse length, the population transfer is negligible and will not affect the two-state dynamics between the $n = 0$ and $+1$ bins. Of the higher-order processes, the four-photon processes are the most likely to

affect the two-state validity. In the case of no center-of-mass motion [$\bar{x}(t)=0$ for all t], the Rabi frequency at the resonance of the $n=0$ to $+2$ transition is [12]

$$\Omega_{\text{Rabi}(0\to+2)} = \frac{U_0^2}{8[\omega_0(0) - \omega_{+1}(0)]} = \frac{U_0^2}{8q^2}. \quad (42)$$

Complete population transfer (for $\kappa=0$) would occur for $\Omega_{\text{Rabi}(0\to+2)}t = \pi$, yielding the additional condition

$$t \ll \frac{8\pi q^2}{U_0^2}. \quad (43)$$

The condition derived equivalently on the $n=-1$ to $+1$ transition is more lenient and therefore, provided that Eqs. (41) and (43) are satisfied, all other transitions can be neglected and the two-state approach is valid.

2. Simplified treatment of the two-state model: Main features of the Bragg spectrum

The two-state model provides approximate Bragg spectra for a condensate with solitary-wave behavior and requires much less computational resources than calculations of the full Gross-Pitaevskii equation. We will demonstrate the success of the two-state solutions to Eq. (36) in Sec. III C. However, the dominant features of the Bragg spectrum can be readily obtained from a particular simplification of the two-state model, which we outline in this section.

Blakie *et al.* [8] have shown that if the optical potential (18) has the simple form $b\cos(\mathbf{q}\cdot\mathbf{R} - \omega t)/2$, then for the case $V(\mathbf{R})=0$ and $C=0$, the detuning in the two-state model is time-independent, i.e.,

$$\Delta_{0\to+1}(\kappa) = q^2 + 2\kappa q - \omega. \quad (44)$$

In that case, the analytic solution to Eq. (36) yields the Bragg spectrum

$$P_{+1}(\omega,t) = \int_{-q/2}^{q/2} \frac{b^2|\phi_0(\kappa,0)|^2}{8\Omega_{\text{Rabi}}^2(\kappa)}[1 - \cos\Omega_{\text{Rabi}}(\kappa)t]d\kappa, \quad (45)$$

where the Rabi frequency is

$$\Omega_{\text{Rabi}}(\kappa) = \sqrt{\left(\frac{b}{2}\right)^2 + \Delta_{0\to+1}^2(\kappa)}. \quad (46)$$

The frequency width of the first-order Bragg transition is

$$\sigma_\omega = \sqrt{b^2 + \left(\frac{\pi}{t}\right)^2}, \quad (47)$$

where contributions from power broadening and temporal broadening are included. In the limit $bt/4 \ll 1$ the total scattered population across the single Bragg resonance is

$$\int_{-\infty}^{\infty} P_{+1}(\omega,t)d\omega = \frac{\pi b^2 t}{8}. \quad (48)$$

For the more general case we are considering here, the optical potential in the translating frame is given in one di-

mension by Eq. (25), which can be expanded as

$$V_{\text{opt}}^t(X,t) = \frac{1}{2}U_0\{\cos(qX - \omega t)\cos[q\bar{x}(t)]$$
$$- \sin(qX - \omega t)\sin[q\bar{x}(t)]\}. \quad (49)$$

In many cases $\cos[q\bar{x}(t)]$ and $\sin[q\bar{x}(t)]$ will be periodic functions of time and can thus be replaced by their respective Fourier series. After some algebraic manipulation Eq. (49) can then be expressed as a linear sum of simple Bragg potentials with the form considered by Blakie *et al.* [8], i.e.,

$$V_{\text{opt}}^t(X,t) = \frac{1}{2}\sum_l c_l \cos[qX - (\omega + \omega_l)t + \epsilon_l]. \quad (50)$$

The strength, relative phase, and resonance position for each term in the sum can be determined once c_l, ϵ_l, and ω_l are known. If the two Fourier series required for the expansion are not exact, or cannot be found analytically, numerical Fourier transform methods can be used.

If the optical potential (25) can be expanded in the form of Eq. (50) then the Bragg spectrum of the solitary-wave condensate will have a discrete number of resonance peaks due to the multiple Bragg terms in the linear sum. When the individual Bragg spectra due to consecutive terms in frequency space overlap, the effect due to simultaneous application of the Bragg fields can be complicated. However, there are particular regimes where each Bragg response labeled by l can be considered as if it were acting independently of the others, and then Eqs. (44)–(48) can be applied to each resonance, and it is straightforward to construct a complete approximate spectrum by summing the Bragg spectra due to each individual term. We refer to this method of calculating approximate spectra as the *independent resonance approach*. The most important case where this approach applies is when the positions of consecutive resonances are separated by more than the widths of those resonances, i.e.,

$$\omega_{l+1} - \omega_l > \frac{\sigma_\omega(c_{l+1}) + \sigma_\omega(c_l)}{2}. \quad (51)$$

Other particular cases arise; for example, in the perturbative limit $c_l t/4 \ll 1$, the independent resonance approach is accurate for Bragg pulse lengths such that all resonances labeled l obey

$$\cos\left[\frac{1}{2}(\omega_{l'} - \omega_l)t - (\epsilon_{l'} - \epsilon_l)\right] = 0 \quad (52)$$

for all other resonances l'.

D. Nonlinear effects

Calculating numerical solutions to the three-dimensional time-dependent Gross-Pitaevskii equation is computationally intensive. Blakie *et al.* [8] demonstrated that within a well-defined parameter regime the analytic results derived for the case $C=0$ provide a good representation of the main behavior observed in the many-body system. For the systems we are considering, where the condensate has solitary-wave

behavior in the absence of the Bragg pulse, the center-of-mass motion of the condensate is independent of the nonlinear strength of the system and, therefore, in the translating frame the validity regime definitions derived by Blakie *et al.* [8] apply.

There are three dominant many-body effects on Bragg scattering. The first is that atomic interactions within the condensate cause the momentum distribution to broaden during free expansion. The time scale for this has been derived to be $t = 7\sqrt{3}/4\mu$ [8] and provided that the Bragg pulse length is shorter than this time scale, the effect of expansion is negligible. The second many-body effect is a shift in the resonance condition of the first Bragg order due to the mean-field. For condensates confined in a three-dimensional harmonic trap the resonant frequency is higher by approximately $4\mu/7$ [8] and this shift can be neglected when $\mu \ll U_0/2$. In addition to these effects, harmonically trapped condensates with a higher chemical potential have a narrower momentum distribution. This arises due to the form of $\xi(\mathbf{R})$, defined by Eq. (6): a broader spatial distribution leads to a narrower momentum distribution. The Bragg spectra for trapped condensates with a higher chemical potential exhibit narrower spectral features and increased peak scattering. These effects were also observed by Blakie *et al.* [8].

In the case where $C=0$ a description of the three-dimensional system can often be simplified to one dimension without loss of generality, as described in Sec. II C. The Gross-Pitaevskii equation, while it is not separable, can also be reduced to a one-dimensional form (e.g., [13–15]). Bragg spectra calculated using a one-dimensional treatment along the axis of the Bragg pulse also generate reasonably accurate results for a nonlinear condensate, as we will see for a particular example in Sec. III D.

III. TIME-AVERAGED ORBITING POTENTIAL TRAP

In this section we calculate Bragg spectra of a condensate accelerating as a solitary wave. The spectra are calculated at various levels of approximation: (i) using the approximate methods described in Sec. II C, (ii) using the full Schrödinger equation (Gross-Pitaevskii equation with $C=0$), and (iii) using the Gross-Pitaevskii equation in both one and two dimensions.

There are a number of examples of solitary-wave behavior of condensates confined by a harmonic trap (see Sec. II A 1). Solitary-wave solutions with constant velocity exhibit Bragg spectra with the same shape as the spectra of the equivalent stationary condensate but simply translated in frequency space by $q\,d\bar{x}(t)/dt$, as can be seen from Eq. (25) or (37). Solitary-wave solutions which accelerate can produce more elaborate Bragg spectra and for this reason we have chosen to use the example of solitary-wave micromotion of a condensate in a time-averaged orbiting potential (TOP) trap to illustrate our methods discussed in Sec. II. In a TOP trap the condensate accelerates in a circular trajectory following the bias field that removes the discontinuity in the trapping potential ([11] and references therein). The micromotion velocity is so high that the structure of the Bragg spectrum can be measured experimentally with moderate frequency reso-

lution. The experimental investigation of Bragg spectra in a TOP trap [6] shows qualitative agreement between the experimental data and calculations made using the one-dimensional Schrödinger equation. Our theoretical methods provide the framework for a detailed understanding of the concepts introduced previously in relation to Bragg spectroscopy in a TOP trap [6,16].

A. Theoretical description of the TOP trap

The TOP trap potential can be well approximated by

$$V_{\mathrm{TOP}}(\mathbf{r},t) = V_{\mathrm{H}}(\mathbf{r}) + r_0(\cos\Omega t, \sin\Omega t, 0) \cdot \mathbf{r}, \quad (53)$$

where r_0 is the so-called "circle of death" radius and Ω is the bias field rotation frequency [11]. Equation (53) is of the form required for solitary-wave solutions to exist [see Eq. (12)] and in fact condensation occurs into the system ground state, which is a solitary-wave solution of the Gross-Pitaevskii equation with circular center-of-mass motion given by

$$\bar{\mathbf{r}}(t) = \gamma(\cos\Omega t, \sin\Omega t, 0), \quad (54)$$

where $\gamma = 2r_0/(\Omega^2 - 1)$ [11].

B. Effective optical potential

The solitary-wave description of condensate micromotion allows Bragg spectroscopy in a TOP trap to be described using the theory presented in Sec. II. In the translating frame the optical potential of the Bragg pulse becomes, in one dimension,

$$V_{\mathrm{opt}}^t(X,t) = \frac{1}{2}U_0\cos(qX + q\gamma_t\cos\Omega t - \omega t). \quad (55)$$

The optical potential of the Bragg pulse, in the moving frame of the condensate, has been identified previously as being a frequency-modulated potential [6,16]. Our discussion in the translating frame provides a theoretical validation of that identification.

In anticipation of interpreting Bragg spectra of a condensate in a TOP trap we decompose the optical potential in the translating frame in the form of Eq. (50). For the frequency-modulated potential of Eq. (55) such an expansion is well known, i.e.,

$$
\begin{aligned}
V_{\mathrm{opt}}^t(X,t) = \frac{1}{2}U_0 \Bigg\{ & J_0(\gamma q)\cos(qX - \omega t) - \sum_{l=0}^{\infty}(-1)^l J_{2l+1}(\gamma q) \\
& \times \Bigg[\cos\left(qX - \omega t - (2l+1)\Omega t - \frac{\pi}{2}\right) \\
& + \cos\left(qX - \omega t + (2l+1)\Omega t - \frac{\pi}{2}\right) \Bigg] \\
& + \sum_{l=1}^{\infty}(-1)^l J_{2l}(\gamma q)[\cos(qX - \omega t + 2l\Omega t) \\
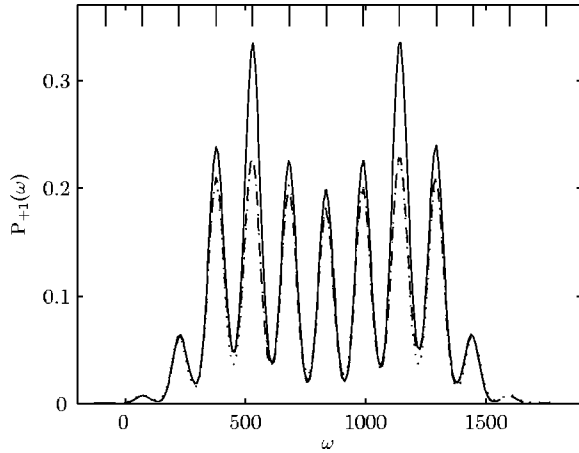& + \cos(qX - \omega t + 2l\Omega t)] \Bigg\},
\end{aligned} \quad (56)
$$

FIG. 1. Bragg spectrum of a condensate in a TOP trap calculated using the full Schrödinger equation (−), the two-state model (−−), and the independent resonance approach (··). The vertical lines along the top of the figure indicate the positions of the spectral resonances predicted by Eq. (56). Parameters are $U_0=45, q=29, r_0 =1241, \Omega=153$, and $t=0.105\pi$ (1 TOP trap cycles).

FIG. 2. Bragg spectrum of a condensate in a TOP trap calculated using the full Schrödinger equation (−), the two-state model (−−), and the independent resonance approach (··). The vertical lines along the top of the figure indicate the positions of the spectral resonances predited by Eq. (56). Parameters are $U_0=45, q=29, r_0 =878, \Omega=76$, and $t=0.092\pi$ (3.5 TOP trap cycles).

where $J_\nu(z)$ is the Bessel function of the first kind of order ν and with argument z. In the translating frame, the condensate is subjected to an optical field which is the sum of simple Bragg terms, separated in frequency by the TOP trap bias field rotation frequency. Therefore, we expect that the Bragg spectra of a condensate with micromotion will have multiple resonances separated by Ω.

C. Bragg spectra

The Bragg spectrum of a condensate in a TOP trap is presented in Fig. 1 for a parameter set which is experimentally accessible [6]. The spectrum calculated using the full Schrödinger equation (i.e., $C=0$) is shown as a solid line. The Bragg spectrum is centered at the first-order Bragg resonance [see Eqs. (39) and (40)] and exhibits additional structure compared to the single resonance peak at $\omega=q^2$ which would be expected from a single Bragg term. Equation (56) correctly predicts the positions of the resonance peaks in the Bragg spectrum (as indicated by the vertical lines in the figure).

We have also generated approximate Bragg spectra of a condensate in a TOP trap using the two-state model (see Sec. II C), as well as the simplified version of the two-state model, the independent resonance approach (see Sec. II C 2). Solving the two-state equation (36) is two orders of magnitude faster than solving the full Schrödinger equation. Provided that the validity conditions of Eqs. (41) and (43) are satisfied, the results of the two-state model are reasonably accurate, as demonstrated by the dashed line in Fig. 1 The main discrepancy between the two-state method and the full $C=0$ calculation is the underestimation of the two strongest resonance peaks. This occurs because the stationary harmonic trap in the translating frame has been neglected in the two-state approach. The effect of the harmonic trap is to shift population toward zero momentum thus allowing more condensate population to be scattered into the $n=+1$ momentum
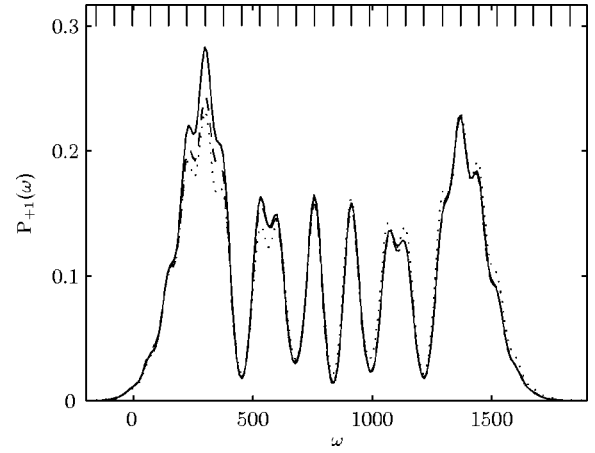
order. The calculation using the independent resonance approach is indicated by the dotted line in Fig. 1 and is almost identical to the Bragg spectrum calculated using the two-state approach. This is because each Bragg resonance within the spectrum is well resolved [refer to Eq. (51)] and, furthermore, the spectrum in Fig. 1 is for exactly eight TOP trap cycles and we note that Eq. (52) holds in that case for TOP trap resonances which are consecutive in frequency space.

Figure 2 shows a Bragg spectrum for a condensate in a TOP trap where the bias field rotation frequency is halved compared with the case of Fig. 1, and the Bragg pulse length is not an integer multiple of the rotation period. The spectrum is again centered at $\omega=q^2$ and the resonances are separated by the TOP trap rotation frequency, although a number of peaks appear missing (including the central one) because their weight is small in expansion (56). In contrast to Fig. 1, the Bragg spectrum of Fig. 2 is no longer symmetric about the center of the first-order Bragg resonance, but favors the low-frequency resonances due to our initial conditions, which yield a negative Doppler term for the first half of the TOP trap rotation. We observe that the two-state model does exhibit the lack of symmetry present in the full Schrödinger equation calculation, while the independent Bragg resonance approach does not. We also note that the two-state model more accurately approximates the full Schrödinger equation calculation than was the case in Fig. 1. The reason for this is that neglecting the harmonic trap has less effect at lower scattered fractions.

D. Effect of condensate nonlinearity

In this section we present Bragg spectra for a nonlinear condensate in a TOP trap calculated using the Gross-Pitaevskii equation in one dimension (the x direction) and in two dimensions (neglecting the z dimension). In each case **q** is taken to be along the x axis and the trapping potential is the appropriate dimensional reduction of Eq. (53). In general
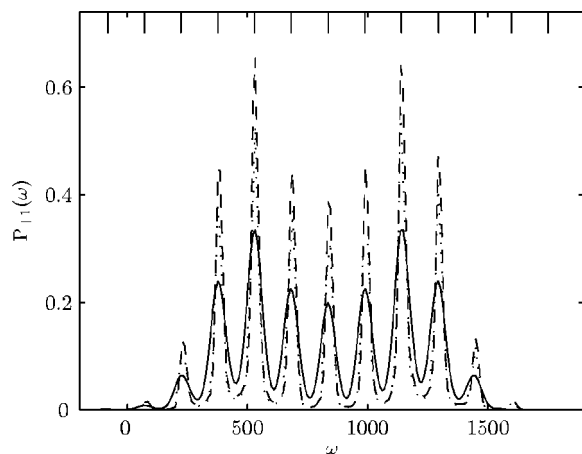
FIG. 3. Bragg spectrum of a condensate in a TOP trap with the parameters of Fig. 1 calculated using the Schrödinger equation (–), the one-dimensional Gross-Pitaevskii equation with $C_{1D}=85$, $\mu=10.08$ (– –), and the two-dimensional Gross-Pitaevskii equation with $C_{2D}=600$, $\mu=9.85$ (··). The vertical lines along the top of the figure indicate the positions of the spectral resonances predicted by Eq. (56).

the Gross-Pitaevskii equation is not separable so we determine the appropriate nonlinear strength in the reduced dimensional system by arranging to have the same chemical potential (and Thomas-Fermi radius) as in the three-dimensional description.

Figure 3 illustrates the Bragg spectra for the same parameters as in Fig. 1 but with $C \neq 0$. The nonlinear strength corresponds to approximately 2×10^4 atoms in the Otago TOP trap [6]. The results from the one-dimensional Gross-Pitaevskii equation agree well with the Bragg spectrum calculated in two dimensions, justifying our simplification of the problem to one dimension. Calculating the two-dimensional Bragg spectra in Fig. 3 is computationally expensive, requiring approximately 10 CPU hours on a 3 GHz Pentium to calculate each point (with 100 points required for the full spectrum).

We have also reproduced in Fig. 3 the result from the linear case of Fig. 1, and comparing the $C=0$ and the C

$\neq 0$ spectra the effects discussed in Sec. II D are observed: the nonlinear Bragg spectra exhibit increased peak scattered fractions, reduced resonance width, and a slight increase in the resonant frequencies, with respect to the equivalent $C =0$ system. The increased resolution in the features of the Bragg spectrum occurs due to the reduced momentum width of the initial state, determined by the form of $\xi(\mathbf{R})$. It is interesting to note that the two-state model can also exhibit narrowed resonances if the initial state is taken to be the same numerically calculated ground state as was used for the full nonlinear Gross-Pitaevskii calculation.

IV. CONCLUSION

We have presented methods for identifying the key features of the Bragg spectrum of a condensate that exhibits solitary-wave behavior. In particular such an accelerating condensate becomes stationary in a translating frame and an effective optical potential contains the only explicit time dependence of the system in that frame. We have generalized the two-state formalism introduced by Blakie *et al.* [8] and have defined the regime in which the approximate spectra generated using that approach are in good agreement with full calculations. Bragg spectra of particular accelerating solitary-wave solutions exhibit multiple resonances and we have identified particular cases where those resonances each act independently of the others, thereby revealing the main features of the Bragg spectrum with minimal calculation.

The Bragg spectrum of a condensate in a TOP trap has been used to illustrate the application of our theory. We have described the resonance structure in the spectra and in the validity regime of our treatment have demonstrated excellent agreement between our approximate methods and full theoretical calculations.

[1] J. Stenger, S. Inouye, A. P. Chikkatur, D. M. Stamper-Kurn, D. E. Pritchard, and W. Ketterle, Phys. Rev. Lett. **82**, 4569 (1999).

[2] S. Richard, F. Gerbier, J. H. Thywissen, M. Hugbart, P. Bouyer, and A. Aspect, Phys. Rev. Lett. **91**, 010405 (2003).

[3] P. B. Blakie and R. J. Ballagh, Phys. Rev. Lett. **86**, 3930 (2001).

[4] H. P. Büchler, P. Zoller, and W. Zwerger, Phys. Rev. Lett. **93**, 080401 (2004).

[5] P. B. Blakie, R. J. Ballagh, and C. W. Gardiner, Phys. Rev. A **65**, 033602 (2002).

[6] R. Geursen, N. R. Thomas, and A. C. Wilson, Phys. Rev. A **68**, 043611 (2003).

[7] K. J. Challis, R. Geursen, R. J. Ballagh, and A. C. Wilson, in *Laser Spectroscopy: Proceedings of the XVI International Conference* (World Scientific, Singapore, 2004), p. 181.

[8] P. B. Blakie and R. J. Ballagh, J. Phys. B **33**, 3961 (2000).

[9] S. A. Morgan, R. J. Ballagh, and K. Burnett, Phys. Rev. A **55**, 4338 (1997).

[10] Dionisios Margetis, J. Math. Phys. **40**, 5522 (1999).

[11] K. J. Challis, R. J. Ballagh, and C. W. Gardiner, Phys. Rev. A **70**, 053605 (2004).

[12] P. Blair Blakie, Robert J. Ballagh, and Charles W. Clark, Phys. Rev. A **68**, 023601 (2003).

[13] E. Kh. Abdullaev and R. Galimzyanov, J. Phys. B **36**, 1099 (2003).

[14] L. Salasnich, A. Parola, and L. Reatto, Phys. Rev. A **69**, 045601 (2004).

[15] A. D. Jackson, G. M. Kavoulakis, and C. J. Pethick, Phys. Rev. A **58**, 2417 (1998).

[16] M. Cristiani, O. Morsch, J. H. Müller, D. Ciampini, and E. Arimondo, Phys. Rev. A **65**, 063612 (2002).